High-Spin Organocobalt(II) Complexes in a Thioether Coordination Environment

Julie A. DuPont, Michael B. Coxey, Peter J. Schebler, Christopher D. Incarvito, William G. Dougherty, Glenn P. A. Yap, Arnold L. Rheingold, and Charles G. Riordan*

Department of Chemistry and Biochemistry, University of Delaware, Newark, Delaware 19716

Received September 8, 2006

A series of electronically and coordinatively unsaturated four-coordinate organocobalt(II) complexes, [PhTt^{tBu}]Co(R) ([PhTt^{tBu}] = phenyltris((*tert*-butylthio)methyl)borate; R = Me, Et, Ph, Bn) have been prepared by reaction of [PhTt^{tBu}]CoCl with the corresponding R_2Mg reagent. These high-spin, $S = 3/2$, complexes have been characterized spectroscopically and several of their structures determined by X-ray diffraction. The R = allyl derivative, [PhTt^{tBu}]Co(η^3-allyl), is low spin. Reaction of [PhTt^{tBu}]Co(R) with CO yielded the acyl adducts [PhTt^{tBu}]Co(CO)C(O)R when R = Me, Et, Ph. These five-coordinate, low-spin complexes possess square pyramidal stereochemistry with a thioether occupying the apical position. In contrast, [PhTt^{tBu}]Co(R), R = Bn or allyl, reacted with CO generating the brown cobalt(I) dicarbonyl [PhTt^{tBu}]Co(CO)$_2$. The latter reaction is proposed to proceed via CO-promoted Co−C bond homolysis. The Ni complex [κ^2-PhTt^{tBu}]Ni(η^3-allyl) shows no reactivity with CO under similar conditions. Each of the [PhTt^{tBu}]Co(R) species reacts with NO, generating brown [κ^2-PhTt^{tBu}]Co(NO)$_2$ in good yield.

Introduction

High-spin organonickel complexes are exceedingly rare,[1] despite their suggested importance in a number of biochemical transformations.[2] It is generally appreciated that the strong donor characteristics of a σ-bonded alkyl are sufficient to drive the nickel to its low-spin configuration. In the context of four-coordinate complexes, the alkyl donor provides impetus for conversion from tetrahedral to square planar stereochemistry.[3] Indeed, we are unaware of any examples of tetrahedral organonickel complexes. Motivated by the lack of such precedents, we embarked on the synthesis of such species several years ago.[4] Utilizing the tridentate ligand phenyltris((*tert*-butylthio)methyl)-borate [PhTt^{tBu}], we attempted to prepare four-coordinate organonickel species via metathetical transformations commencing with [PhTt^{tBu}]NiCl. Regardless of the source of the alkyl (or aryl) nucleophile, the reactions led to the formation of a thiametallacycle, [κ^2-PhTt^{tBu}]Ni[η^2-CH$_2$SBu^t], via a ligand degradation pathway involving cleavage of the B−CH$_2$ bond.[4] Reasoning that the product was formed via the intermediacy of the unstable organonickel species [PhTt^{tBu}]Ni(R), low-temperature analysis and chemical interception of this species were attempted. Low-temperature proton NMR investigations showed no evidence of the suggested intermediate despite our expectation that the species would have efficient electron spin relaxation characteristics and, thus, be amenable to study via this technique. In the case of chemical trapping, low-temperature alkylation of [PhTt^{tBu}]NiCl in the presence of PR_3, CO, or CNBu^t led only to the Ni$^+$ complexes [PhTt^{tBu}]Ni(L).[4] Therefore, we were left to conclude that organonickel intermediates were not formed in these reactions. Electron transfer generating Ni$^+$ species was proposed as the most probable mechanism. Support for this conclusion was provided by the observation that Na/Hg reduction of [PhTt^{tBu}]NiCl led to [κ^2-PhTt^{tBu}]Ni[η^2-CH$_2$SBu^t] or [PhTt^{tBu}]Ni(L), the latter if a trapping ligand was provided.

Scheme 1. Synthesis of [PhTt^{tBu}]Co(R) Complexes

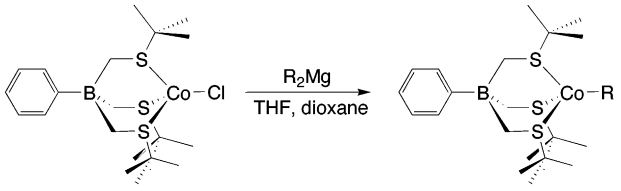

R = Me, Et, Ph, Bn, allyl

Simultaneously, we examined similar transformations at cobalt expecting the organocobalt complexes to be inherently more stable.[4] Metathetical reactions between [PhTt^{tBu}]CoCl and R_2Mg reagents proceeded smoothly to the desired [PhTt^{tBu}]Co(R). Despite their electronic and coordinative unsaturation, these complexes are stable even with respect to β-hydrogen elimination. This stability has been documented for related [Tp^R]Co(R) complexes prepared independently by the Theopold[5] and Akita[6−8] laboratories. The stability of the [Tp^{tBu,Me}] derivatives may have some steric origin, as the ligand cone angle generally limits access to five-coordinate complexes, e.g., [Tp^{tBu,Me}]Co(H)(olefin), requisite for β-hydrogen elimination. Consequently, the [Tp^{tBu}] and [Tp^{tBu,Me}] ligands have been termed "tetrahedral enforcers". The high-spin nature of the complexes provides an electronic explanation for their stability, as detailed by Akita.[8]

* Corresponding author. E-mail: riordan@udel.edu.

(1) For example, (a) D'Aniello, M. J.; Barefield, E. K. *J. Am. Chem. Soc.* **1976**, *98*, 1610. (b) Lin, S.-K.; Juan, B. *Helv. Chim. Acta* **1991**, *74*, 1725.

(2) (a) Ragsdale, S. W.; Riordan, C. G. *J. Biol. Inorg. Chem.* **1996**, *1*, 489. (b) Hinderberger, D.; Piskorski, R. R.; Goenrich, M.; Thauer, R. K.; Schweiger, A.; Harmer, J.; Jaun, B. *Angew. Chem.* **2006**, *45*, 3602.

(3) Cotton, F. A.; Wilkinson, G.; Murillo, C. A.; Bochmann, M. *Advanced Inorganic Chemistry*, 6th ed.; John Wiley & Sons, Inc.: New York, 1999; p 845.

(4) Schebler, P. J.; Mandimutsira, B. S.; Riordan, C. G.; Liable-Sands, L.; Incarvito, C. D.; Rheingold, A. L. *J. Am. Chem. Soc.* **2001**, *123*, 331.

(5) Jewson, J. D.; Liable-Sands, L. M.; Yap, G. P. A.; Rheingold, A. L.; Theopold, K. H. *Organometallics* **1999**, *18*, 300.

(6) Akita, M.; Shirasawa, N.; Hikichi, S.; Moro-oka, Y. *Chem. Commun.* **1998**, 973.

(7) Shirasawa, N.; Akita, M.; Hikichi, S.; Moro-oka, Y. *Chem. Commun.* **1999**, 417.

(8) Shirasawa, N.; Nguyet, T. T.; Hikichi, S.; Moro-oka, Y.; Akita, M. *Organometallics* **2001**, *20*, 3582.

10.1021/om0608253 CCC: $37.00
Publication on Web 01/17/2007

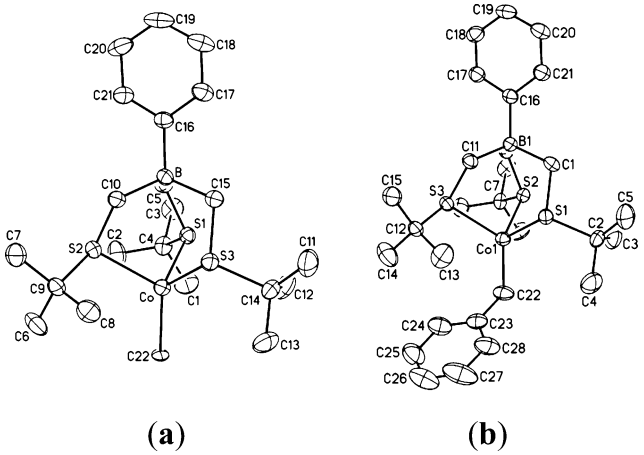

Figure 1. Thermal ellipsoid plots of (a) [PhTt^{tBu}]Co(Me) and (b) [PhTt^{tBu}]Co(Bn). Thermal ellipsoids are drawn at 30% probability. Hydrogen atoms have been omitted for clarity.

The molecular orbital required to accept the hydrogen in the β-hydrogen elimination reaction must be empty. The high-spin state ensures that the symmetry-appropriate orbitals are half-filled.

Herein, we describe the preparation, characterization, and structures of a series of [PhTt^{tBu}]Co(R) complexes. Subsequent reactivity with CO demonstrates that the course of the reaction depends on the identity of the organometalloid fragment. When R = Me, Et, or Ph, CO insertion leads to the five-coordinate acyl complexes [PhTt^{tBu}]Co(C(O)R)(CO). Alternatively, for R = Bn or allyl, reduction is the predominant pathway, as evidenced by the formation of [PhTt^{tBu}]Co(CO)$_2$. Reaction of [PhTt^{tBu}]Co(R) with NO generated [κ^2-PhTt^{tBu}]Co(NO)$_2$ regardless of the identity of R. Direct synthesis of a low-spin organonickel complex, [κ^2-PhTt^{tBu}]Ni(η^3-allyl), was achieved using (allyl)$_2$Mg.

Detailed studies by Peters[9] on related Co^{2+} complexes supported by the [PhB(CH$_2$PPh$_2$)$_3$] ligand have demonstrated that strong field ligands combined with axial distortion in a pseudo-tetrahedral stereochemistry can lead to a low-spin ground state. All of the four-coordinate complexes reported here are high-spin, consistent with expectation that the ligand field afforded by [PhTt^{tBu}] is weaker than that of [PhB(CH$_2$PPh$_2$)$_3$].

Results and Discussion

(i) Synthesis and Characterization of Organocobalt(II) Complexes [PhTt^{tBu}]Co(R) (R = Me, Et, Ph). Addition of the appropriate Grignard reagent to THF/1,4-dioxane solutions of the chloride starting material [PhTt^{tBu}]CoCl produced a rapid color change from blue to green, indicating conversion to the organocobalt species [PhTt^{tBu}]Co(R) (R = Me, Et, Ph) with concomitant formation of a white solid, $MgX_2 \cdot C_4H_8O_2$. The precipitate was removed by filtration. Subsequently, the solvent was reduced in vacuo, leaving a green solid. The product was extracted with pentane to afford the organocobalt(II) complexes in modest yields (63−78%; see Scheme 1). These high-spin, paramagnetic complexes are thermally stable to temperatures up to 60 °C, but decompose rapidly upon exposure to air or moisture. The molecular structure of the methyl derivative was determined by X-ray diffraction, Figure 1a, with associated analysis data contained in Table 1 and selected bond distances and angles in Table 2. [PhTt^{tBu}]Co(Me) features an approximate C_3 symmetry with the methyl carbon resting on the noncrystallographically imposed 3-fold axis that is defined by the B−Co vector of the [PhTt^{tBu}]Co fragment (B−Co−C, 178.9°). The cobalt−carbon bond length of 2.052(3) Å is consistent with other tetrahedral organocobalt complexes in a sterically hindered environment[5,8] as well as other Co^{2+} alkyl complexes, e.g., (TMEDA)Co(CH$_2$SiMe$_3$)$_2$ and (TMEDA)Co(CH$_2$CMe$_3$)$_2$.[10] However, it is 0.05 Å shorter than the cobalt−carbon bond length reported by Theopold for [Tp^{tBu}]Co(Me).[5] This shorter bond length for [PhTt^{tBu}]Co(Me) as compared to the Tp^{tBu} analogue is indicative of differences in the electronic properties of the respective borato ligands. Specifically, the [Tp^{tBu}] ligand is more electron donating than the [PhTt^{tBu}], resulting in a more electron-rich metal fragment. This is borne out not only in the cobalt−carbon bond lengths but also in comparison of the infrared spectra of the cobalt monocarbonyl species of each ligand system. The infrared spectrum of [PhTt^{tBu}]Co(CO) reveals the CO stretch at 1966 cm^{-1}, while the more electron-rich [Tp^{tBu}]-Co(CO) shows a lower energy stretch at 1950 cm^{-1}.[11]

The organocobalt complexes were also characterized by NMR and electronic absorption spectroscopic methods. The paramagnetic ^{1}H NMR spectrum of [PhTt^{tBu}]Co(Me) exhibits a broad resonance assigned to the *tert*-butyl protons at δ 3.16. The phenyl protons resonate at δ 18.9 (*o*-phenyl), δ 10.8 (*m*-phenyl), and δ 9.8 (*p*-phenyl). The resonance for the methyl moiety was not observed, and it is presumed to be broadened into the baseline by the proximity to the paramagnetic cobalt. The ethyl and phenyl derivatives displayed similar ^{1}H NMR spectra, with the broad *tert*-butyl resonances found at δ 1.22 and 3.35, respectively. An upfield signal at δ −9.36 was assigned to the −C*H*$_3$ resonance of the ethyl moiety. The upfield signal of the −C*H*$_3$ is similar to that observed for the related [Tp^{iPr2}]Co(Et) (δ −16).[7] For [PhTt^{tBu}]Co(Ph), the *meta* protons of the Co(Ph) were found shifted downfield at δ 40.4, while the *para* and *ortho* protons were assigned to upfield resonances at δ −20.9 and −26.5, respectively. These assignments are made on the basis of signal integration and chemical shift, the latter relative to the diamagnetic region. Specifically, due to π spin delocalization in aromatic ligands, the *meta* protons shift downfield, whereas the *ortho* and *para* protons are found upfield. The upfield signals are differentiated on the basis of signal integration.[12] For example, shifts of similar sign and magnitude are observed for the aryl ligand of [Ni(tmc)SPh](OTf)[13] and Fe(OEP)Ph.[14]

The electronic spectra of the organocobalt complexes are consistent with a high-spin d^7 metal center in a tetrahedral ligand field. For [PhTt^{tBu}]Co(Me), two d−d transitions are evident at λ_{max} (ϵ, M^{-1} cm^{-1}) 632 (537) and 725 (574) nm. These values are similar to those found for [PhTt^{tBu}]CoCl and related [Tp^R]-Co(R) complexes. Generally, [Tp^R]CoX species display transitions of $\epsilon > 300$ in the 500−600 nm range. The transitions were assigned by following the energy diagram reported by Ciampolini.[15] Thus, the transition at 632 nm has been assigned to $^4A_2 \rightarrow {}^4T_1(P)$, and the higher energy transition at 724 nm

(9) Jenkins, D. M.; Bilio, A. J. D.; Allen, M. J.; Betley, T. A.; Peters, J. C. *J. Am. Chem. Soc.* **2002**, *124*, 15336.

(10) Hay-Motherwell, R. S. W. G.; Hussain, B.; Hursthouse, M. B. *Polyhedron* **1990**, *9*, 931.

(11) Detrich, J. L.; Konecny, R.; Vetter, W. M.; Doren, D.; Rheingold, A. L.; Theopold, K. H. *J. Am. Chem. Soc.* **1996**, *118*, 1703.

(12) Baidya, N.; Olmstead, M.; Mascharak, P. K. *Inorg. Chem.* **1991**, *30*, 939.

(13) Ram, M. S.; Riordan, C. G.; Ostrander, R.; Rheingold, A. L. *Inorg. Chem.* **1995**, *34*, 5884.

(14) Cocolios, P.; Lagrange, G.; Guilard, R. *J. Organomet. Chem.* **1983**, *253*, 65.

(15) Ciampolini, M.; Nardi, N.; Orioli, P. L. *J. Chem. Soc., Dalton Trans.* **1984**, 2265.

Table 1. Crystallographic Data for [κ^2-PhTt^{tBu}]Ni(η^3-allyl) (1), [PhTt^{tBu}]Co(Me) (2), [PhTt^{tBu}]Co(Bn) (5), [PhTt^{tBu}]Co(η^3-allyl) (6), [PhTt^{tBu}]Co(CO)(C(O)Me) (7), [PhTt^{tBu}]Co(CO)(C(O)Et) (8), [PhTt^{tBu}]Co(CO)(C(O)Ph) (9), [PhTt^{tBu}]Co(CO)$_2$ (10), and [PhTt^{tBu}]Co(NO)$_2$ (12)

	1	2	5	6	7	8	9	10	12
formula	$C_{24}H_{43}S_3BNi$	$C_{22}H_{41}S_3BCo$	$C_{28}H_{45}S_3BCo$	$C_{24}H_{43}S_3BCo$	$C_{24}H_{41}S_3O_2BCo$	$C_{25}H_{43}S_3O_2BCo$	$C_{29}H_{43}S_3O_2BCo$	$C_{23}H_{38}S_3O_2BCo$	$C_{21}H_{38}S_3N_2O_2BCo$
fw	497.28	471.47	547.56	497.50	527.49	541.51	589.55	512.45	516.45
color, habit	yellow, plates	green, blocks	brown, plates	brown, needles	red, blocks	red, blocks	red, plates	brown, needles	red, plates
cryst syst	monoclinic	monoclinic	monoclinic	monoclinic	triclinic	triclinic	monoclinic	monoclinic	monoclinic
space group	*P*2(1)/*n*	*P*2(1)/*n*	*P*2(1)/*c*	*P*2(1)/*n*	*P*$\bar{1}$	*P*$\bar{1}$	*P*2(1)/*n*	*P*2(1)/*n*	*P*2(1)/*e*
a, Å	9.9823(9)	9.7856(2)	15.262(4)	9.619(1)	11.1858(3)	10.4639(1)	9.425(4)	10.04(1)	11.6709(8)
b, Å	11.4566(1)	21.6045(4)	10.502(2)	22.827(2)	11.4379(3)	110.7108(1)	22.870(9)	20.95(3)	11.9956(8)
c, Å	23.248(2)	12.6512(2)	19.279(4)	12.437(1)	13.2639(3)	12.579(1)	14.474(7)	12.78(2)	19.385(1)
α, deg	90	90	90	90	111.406(1)	79.721(2)	90	90	90
β, deg	95.353(2)	99.1316(5)	105.982(4)	99.575(2)	97.879(1)	80.553(2)	101.356(8)	101.35(3)	95.593(1)
γ, deg	90	90	90	90	113.333(1)	82.265(2)	90	90	90
V, Å^3	2647.1(4)	2640.73(8)	2970.7(1)	2692.8(5)	1369.74(6)	1410.6(2)	3059(2)	263.5(7)	2700.9(3)
Z	4	4	4	4	2	2	4	4	4
T, K	150	295	223	150	173	173	223	218	173
D_{calcd}, g/cm^{-1}	1.248	1.186	1.224	1.227	1.279	1.275	1.28	1.292	1.27
2θ range, deg	1.98−28.29	1.88−25.00	2.20−26.00	1.78−28.26	2.08−28.33	1.66−28.31	1.69−25.99	2.37−28.30	1.75−28.30
μ (Mo Kα), mm^{-1}	0.978	0.892	0.803	0.879	0.873	0.850	0.79	0.906	0.886
R1, wR2	0.0423, 0.0881	0.0499, 0.1156	0.0804, 0.1905	0.0561, 0.0923	0.0337, 0.0882	0.0296, 0.0937	0.0849, 0.1960	0.0610, 0.1485	0.0399, 0.0951

Table 2. Selected Bond Lengths and Bond Angles for [PhTt^{tBu}]Co(Me) and [PhTt^{tBu}]Co(Bn)

length (Å)			angle (deg)
	[PhTt^{tBu}]Co(Me) (**2**)		
Co−C(22)	2.052(3)	C(22)−Co−S(1)	121.0(1)
Co−S(1)	2.341(1)	C(22)−Co−S(2)	119.5(1)
Co−S(2)	2.341(1)	C(22)−Co−S(3)	119.5(1)
Co−S(3)	2.352(1)		
	[PhTt^{tBu}]Co(Bn) (**5**)		
Co−C(22)	2.015(5)	C(22)−Co−S(1)	122.5(2)
Co−S(1)	2.348(1)	C(22)−Co−S(2)	113.4(1)
Co−S(2)	2.338(1)	C(22)−Co−S(3)	126.2(1)
Co−S(3)	2.366(1)		

has been assigned to $^4A_2 \rightarrow {}^4T_1(F)$. In accord with the enhanced ligand field strength of the ethyl donor, the band for [PhTt^{tBu}]-Co(Et) is shifted ca. 25 nm to a lower wavelength when compared to that of [PhTt^{tBu}]Co(Me), while the band for [PhTt^{tBu}]Co(Ph) is shifted ca. 10 nm to a higher wavelength, indicating the expected decrease in ligand field strength for the phenyl moiety when compared to that of [PhTt^{tBu}]Co(Me). Each organocobalt complex in this series demonstrates a less intense d−d band than the starting material, [PhTt^{tBu}]CoCl, due to the enhanced ligand field strengths of the alkyl and phenyl moieties compared to that of the halide.

The high-spin, tetrahedral configuration of these 15 e$^-$ complexes was confirmed by magnetic moment measurements. Room-temperature values of 4.1−5.1 μ_B were determined in solution by the Evans method. These values are in accord with a quartet state, $S = 3/2$. While these values are larger than anticipated for a spin-only contribution, 3.9 μ_B, contributions from angular momentum are anticipated for this class of complexes, e.g., [Tp$^{R'}$]Co(R).[5,8,16]

(ii) Synthesis, Characterization, and Molecular Structure of [PhTt^{tBu}]Co(Bn). Reaction of [PhTt^{tBu}]CoCl with BnMgBr in THF/1,4-dioxane solution resulted in a rapid color change from blue to deep red-purple with formation of a white precipitate, $MgX_2 \cdot C_4H_8O_2$. The reaction mixture was filtered and solvent was removed under reduced pressure. The product, [PhTt^{tBu}]Co(Bn), was afforded in 55% yield following extraction into pentane. Similar to the other [PhTt^{tBu}]Co(R) complexes, [PhTt^{tBu}]Co(Bn) is thermally stable up to 60 °C, but rapidly decomposes upon exposure to air or moisture.

The room-temperature ^{1}H NMR spectrum of [PhTt^{tBu}]Co-(Bn) contains a single, broad resonance for the three *tert*-butyl groups at δ 2.5, while the phenyl protons of the borato ligand were found at δ 19.3, 11.2, and 10.3. The resonance for the methylene protons of the benzyl moiety were not observed, as it is presumed broadened into the baseline due to its proximity to the paramagnetic center, as was observed for the methyl and ethyl derivatives (vide supra). The *meta* benzyl protons were shifted significantly downfield, at δ 46.4, while the *ortho* and *para* benzyl protons were shifted upfield, δ −93.1 and −110.8, respectively. The high-spin, $S = 3/2$, state was confirmed by the magnetic moment, $\mu_{eff} = 3.9\ \mu_B$. This value is consistent with the magnetic moments measured for other [PhTt^{tBu}]Co(R) complexes, as well as those found for [Tp^{Me3}]Co($CH_2C_6H_5$-*p*-Me)[6] (3.9 μ_B) and [Tp^{iPr2}]Co(α-napthylmethyl)[6] (4.2 μ_B).

The electronic absorption spectrum of [PhTt^{tBu}]Co(Bn) contains a strong absorption band at λ_{max} (ϵ, M^{-1} cm^{-1}) 352 (873) and d−d bands at 514 (681) and 762 (428) nm. The d−d bands were assigned to the $^4A_2 \rightarrow {}^4T_1(P)$ (514 nm) and $^4A_2 \rightarrow {}^4T_1(F)$ (762 nm) transitions, respectively. The first d−d transition

(16) Shriver, D. F.; Atkins, P.; Langford, C. H. *Inorganic Chemistry*, 2nd ed.; W. H. Freeman and Co.: New York, 1994.

Table 3. Selected Bond Lengths and Angles for [PhTt^{tBu}]Co(η^3-allyl)) and [κ^2-PhTt^{tBu}]Ni(η^3-allyl)

	length (Å)		angle (deg)
	[PhTt^{tBu}]Co(η^3-allyl) (**6**)		
Co−C(22)	2.099(2)	C(22)−Co−C(24)	70.25(9)
Co−C(23)	1.997(2)	S(1)−Co−S(2)	92.30(2)
Co−C(24)	2.114(2)	S(1)−Co−S(3)	93.52(2)
Co−S(1)	2.2664(6)	S(2)−Co−S(3)	89.59(2)
Co−S(2)	2.2835(8)	S(2)−Co−C(24)	104.44(7)
Co−S(3)	2.4083(8)		
C(22)−C(23)	1.410 (3)		
C(24)−C(23)	1.382(3)		
	[κ^2-PhTt^{tBu}]Ni(η^3-allyl) (**1**)		
Ni−C(22)	2.021(3)	C(22)−Ni−C(24)	72.1(1)
Ni−C(23)	1.982(3)	S(2)−Ni−S(3)	94.59(3)
Ni−C(24)	2.021(3)	C(22)−C(23)−C(24)	120.5(2)
Ni−S(2)	2.2075(7)		
Ni−S(3)	2.2325(7)		
C(22)−C(23)	1.388(4)		
C(24)−C(23)	1.372(4)		

is blue-shifted ca. 100 nm to higher energy when compared to the other [PhTt^{tBu}]Co(R) complexes (R = Me, Et, Ph), Table 3. This result indicates the enhanced ligand field strength of the benzyl moiety as compared to the alkyl and phenyl moieties. This difference accounts for the complex's purple color.

Crystals appropriate for X-ray diffraction were grown by slow evaporation of a concentrated pentane solution. The molecular structure shows that the Bn moiety is bound in an η^1-fashion, Figure 1b. Selected bond lengths and angles are contained in Table 2. While the Co−C bond length is comparable to other Co^{2+} benzyl complexes found in the literature,[6] the Co−C bond length of 2.015(5) Å is shorter than that in [PhTt^{tBu}]Co(Me), 2.052(3) Å, although it is noted that the diffraction data were collected at different temperatures, 223 and 295 K, respectively. This observation is counterintuitive and in contrast to other Co−Me versus Co−Bn bond distances for 18-electron complexes at parity of supporting ligands. For example, Co−Me = 1.999 Å in MeCo(dmgH)$_2$py versus Co−Bn = 2.065 Å in BnCo(dmgH)$_2$py.[17] It is of interest that the Co−Me bond distance in the isoelectronic [Tp^{tBu}]Co(Me) is also rather long, 2.112(23) Å. One of the S−Co−C angles in [PhTt^{tBu}]Co(Bn) is smaller than the other two (113.4(1)° compared to 122.5(2)° and 126.2(1)°). This differential indicates a clear deviation from C_3 symmetry. Akita and co-workers observed a similar distortion in [Tp^R]Co-benzyl type complexes, [Tp^{Me3}]Co(CH$_2$C$_6$H$_4$-*p*-Me) and [Tp^{iPr2}]Co(α-napthylmethyl). This distortion away from ideal C_3 symmetry is due to a weak interaction between the benzyl moiety and the cobalt metal center. Specifically, when the benzyl moiety is bound in an η^1-fashion, the filled σ-type orbital of the benzyl interacts with the d_{xz} orbital of the cobalt, essentially stabilizing the electron-deficient cobalt center and simultaneously causing a distortion away from ideal C_3 symmetry and, perhaps, shortening the Co−C bond length.[8]

(iii) Synthesis and Characterization of Cobalt and Nickel Allyl Complexes, [PhTt^{tBu}]M(η^3-allyl). Reaction of [PhTt^{tBu}]-CoCl with 2 equiv of allylMgBr in a THF/1,4-dioxane solution produced an immediate color change from a blue to orange with formation of a white precipitate, $MgX_2 \cdot C_4H_8O_2$. Extraction with pentane afforded [PhTt^{tBu}]Co(η^3-allyl) in 62% yield.

Crystals appropriate for X-ray diffraction were grown by slow evaporation from a concentrated pentane solution. A thermal ellipsoid representation of [PhTt^{tBu}]Co(η^3-allyl) is contained in Table 3 with selected bond lengths and angles in Figure 2a. The most notable feature of the structure is the η^3-allyl ligation leading to a square pyramidal Co^{2+} stereochemistry with two basal and one apical thioether.

The absorption spectrum of brown-red [PhTt^{tBu}]Co(η^3-allyl) differs from those of the other [PhTt^{tBu}]Co(R) complexes. In the visible region, a single d−d transition at λ_{max} (ϵ, M^{-1} cm^{-1}) 713 (277) nm is evident. The Evans method magnetic moment was established to be 2.5 μ_B and suggests a low-spin ($S = 1/2$) state with one unpaired electron consistent with the square pyramidal geometry.

In a similar fashion, [PhTt^{tBu}]NiCl was reacted with allylMgBr in THF/1,4-dioxane, producing a rapid color change from red to yellow. The product, [κ^2-PhTt^{tBu}]Ni(η^3-allyl), was isolated in good yield following pentane extraction. The diamagnetic allylnickel derivative is stable with respect to air and moisture. Subsequent investigations revealed that [κ^2-PhTt^{tBu}]Ni(η^3-allyl) is unreactive toward CO. This observation stands in contrast to the reaction of [PhTt^{tBu}]Co(η^3-allyl) with CO under similar conditions, vide infra.

The diamagnetic ^{1}H NMR spectrum of [κ^2-PhTt^{tBu}]Ni(η^3-allyl) exhibits a very broad singlet at δ 1.37, which corresponds to all of the *tert*-butyl protons. This indicates that although the ligand is κ^2, the thioether arms are undergoing rapid exchange on the NMR time scale. The η^3-coordination of the allyl moiety is highlighted by the three signals δ 4.50, 3.30−3.22, and 3.05−3.02 for the CH, *syn*-CH$_2$, and *anti*-CH$_2$ positions, respectively.

Crystals appropriate for X-ray diffraction were grown by slow evaporation from a concentrated diethyl ether solution. A thermal ellipsoid representation of the molecular structure and selected bond lengths and angles are shown in Figure 2a and Table 2, respectively. In contrast to the cobalt analogue, only two of the thioether arms of the borato ligand are bound to the metal center in the nickel complex. The allyl moiety is bound in an η^3-fashion, acting as a four-electron donor.

Related allylnickel complexes supported by [Tp^R] ligands have been synthesized and characterized structurally. Akita and co-workers prepared [Tp^{iPr2}]Ni(η^3-allyl),[8] while Lehmkuhl and co-workers synthesized [Tp]Ni(η^3-allyl).[18] Whereas the [PhTt^{tBu}] derivative is square planar, the [Tp^R] complexes exhibit square pyramidal geometry with all three nitrogen donors coordinated. The apical Ni−N distance in these complexes is longer than that found for the equatorial Ni−N bond distances. The disparity in the binding mode between the [PhTt^{tBu}] and the [Tp^R] allylnickel arises from differences between the sulfur and nitrogen ligands. Specifically, the sulfur ligands in [PhTt^{tBu}] are weaker donors, and therefore, no further electronic stabilization is gained from binding of the third thioether to the nickel.

Reactivity of [PhTt^{tBu}]Co(R) (R = Me, Et, Ph) with CO. In order to investigate the reactivity of the organocobalt(II) complexes, the above-mentioned compounds were exposed to 1 atm of carbon monoxide in pentane, Scheme 2. A dramatic color change from green to red was apparent. For the ethyl complex, one might expect β-hydrogen elimination upon reaction with CO, as this is a common decomposition route for electronically and coordinatively unsaturated compounds.[5,8,19] However, [PhTt^{tBu}]Co(Et) is resistant to β-hydrogen elimination, and reaction of this complex as well as the methyl and phenyl derivatives with CO yields the respective acyl/carbonyl species

(17) (a) Bigotto, A.; Zangrando, E.; Randaccio, L. *J. Chem. Soc., Dalton Trans.* **1976**, 96. (b) Bresciani-Pahor, N.; Randaccio, L.; Zangrando, E.; Antolini, L. *Acta Crystallogr. Sect. C* **1988**, *C44*, 2052.

(18) Lehmkuhl, H.; Naser, J.; Mehler, G.; Keil, T.; Danowki, F.; Benn, R.; Mynott, R.; Schroth, G.; Gabor, B.; Kruger, C.; Betz, P. *Chem. Ber.* **1991**, *124*, 441.

(19) Falbe, J. *Carbon Monoxide in Organic Synthesis*; Springer-Verlag: New York, 1970.

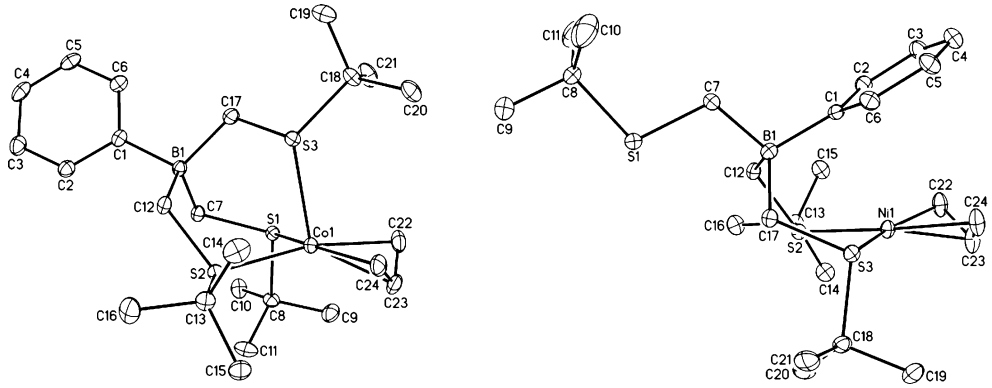

(**a**) (**b**)

Figure 2. Thermal ellipsoid plots of (a) [PhTt^{tBu}]Co(η^3-allyl) and (b) [κ^2-PhTt^{tBu}]Ni(η^3-allyl). Thermal ellipsoids are drawn at 30% probability. Hydrogen atoms have been omitted for clarity.

Scheme 2. Synthesis of [PhTt^{tBu}]Co(CO)(C(O)R) (R = Me, Et, Ph)

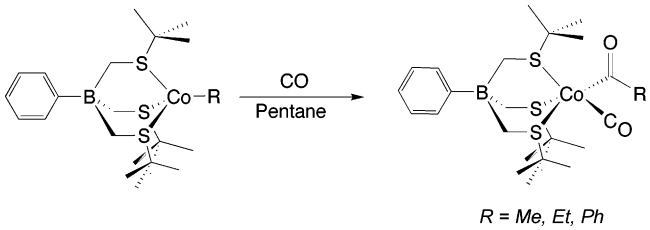

[PhTt^{tBu}]Co(CO)(C(O)R) in good yields. The products were crystallized via slow evaporation from concentrated pentane solutions.

Thermal ellipsoid plots of [PhTt^{tBu}]Co(CO)(C(O)R) (R = Me, Et, Ph) are shown in Figure 3a−c, respectively, with selected bond lengths and angles listed in Table 4. Each complex contains a five-coordinate Co^{2+} within an approximate square pyramidal ligand environment. The carbonyl and acyl ligands lie in the basal plane along with two of the thioether donors. The apical site is occupied by the remaining thioether donor. The three Co−S distances are similar within each complex, with the benzoyl derivative possessing the shortest bond distances, indicating that the electron-withdrawing characteristics of this substituent exert a greater influence than its larger size.

Each of the acyl complexes possesses stereochemistry close to that of an idealized square pyramid. Their τ values are 0.17, 0.04, and 0.03 for R = Me, Et, and Ph, respectively, where values of 0 (square pyramid) and 1 (trigonal bipyramid) set the limits of the Reedijk trigonality index.[20]

As seen in the solid-state structures of the [PhTt^{tBu}]Co(CO)(C(O)R) (R = Me, Et, Ph) complexes, two distinct acyl rotamers are possible. The methyl and ethyl derivatives adopt an *anti* conformation with the acyl oxygen *anti* with respect to the apical sulfur, while the phenyl derivative adopts the opposite conformation with the acyl oxygen *syn* with respect to the apical sulfur. The smaller alkyl substituents of the methyl and ethyl derivatives are able to adopt the *anti* conformation. Apparently, this conformation is not available, however, to the phenyl derivative, due to the steric interaction between one of the *tert*-butyl groups of the ligand and the phenyl ring of the benzoyl moiety. Thus, this complex adopts the opposite conformation. Infrared spectral data indicate that while the methyl derivative adopts the *anti* conformation in solution, two rotamers are present (vide infra).

(20) Addison, A. W.; Rao, T. N.; Reedijk, J.; Vanrijn, J.; Verschoor, G. C. *J. Chem. Soc., Dalton Trans.* **1984**, 1349.

The infrared spectrum of [PhTt^{tBu}]Co(CO)(C(O)Me) recorded in a pentane solution contains ν_{CO} features at 1993, 1684, and 1663 cm^{-1}. The intense high-energy band is assigned to the terminal CO ligand, while the weaker lower energy bands are ascribed to acyl ν_{CO} modes. As stated above, the presence of two acyl rotamers in solution gives rise to the two acyl modes. In contrast, [PhTt^{tBu}]Co(CO)(C(O)Et) and [PhTt^{tBu}]Co(CO)(C(O)Ph) exhibit single acyl ν_{CO} modes at 1658 and 1709 cm^{-1}, respectively, consistent with the single rotoamers observed by X-ray diffraction. The crystallized ethyl derivative adopts the conformation of the less bulky methyl derivative, while the bulky phenyl adopts the alternate conformation.

Expectedly, the change in coordination number and spin state upon reaction with CO changes the electronic spectra of these complexes. Whereas the tetrahedral organocobalt complexes display two visible bands in the 500−600 nm region, giving rise to the green color, the acyl/carbonyl species showed two weaker and lower energy d−d bands. In the spectrum of [PhTt^{tBu}]Co(CO)(C(O)Me), Figure 2, two d−d bands are present at 555 (420) and 689 (175) nm. These arise from $^2A_1 \rightarrow {}^2A_2$ and $^2A_1 \rightarrow {}^2B_2$ transitions, respectively. The propionyl and benzoyl derivatives displayed similar electronic spectra typical of low-spin, d^7 Co^{2+} in a square pyramidal environment. The doublet spin state of these complexes was confirmed by magnetic moment measurements, values of 1.9−2.1 μ_B being obtained for the three complexes.

Reactivity of [PhTt^{tBu}]Co(R) (R = Bn, allyl) Species with CO. Exposure of a pentane solution of [PhTt^{tBu}]Co(R) (R = Bn, allyl) to 1 atm of carbon monoxide resulted in a color change from purple (benzyl) or red-brown (allyl) to the dark brown Co^+ dicarbonyl [PhTt^{tBu}]Co(CO)$_2$, Scheme 3. The product was isolated in 80% yield and crystallized via slow evaporation from a concentrated pentane solution.

This reactivity is distinct from that of the other [PhTt^{tBu}]Co(R) complexes that undergo CO migratory insertion, forming the five-coordinate acyl/carbonyl complexes. Here, the benzyl and allyl complexes undergo homolytic cleavage of the cobalt−carbon bond, formally reducing the metal fragment to Co^+, which is subsequently trapped by CO. Akita reported that carbonylation of [Tp^{iPr2}]Co(R) (R = allyl, *p*-methylbenzyl) results in the formation of the acyl/carbonyl species, which decomposes rapidly to a presumed [Tp^{iPr2}]Co(CO)[8] species, although the latter complex could not be isolated. Alternatively, as detailed by Theopold, [Tp^{tBu}]Co(Me) reacted with CO, generating [Tp^{tBu}]Co(CO).[11] It was argued that [Tp^{tBu}]Co(Me) undergoes bond homolysis due to the large cone angle (268°)

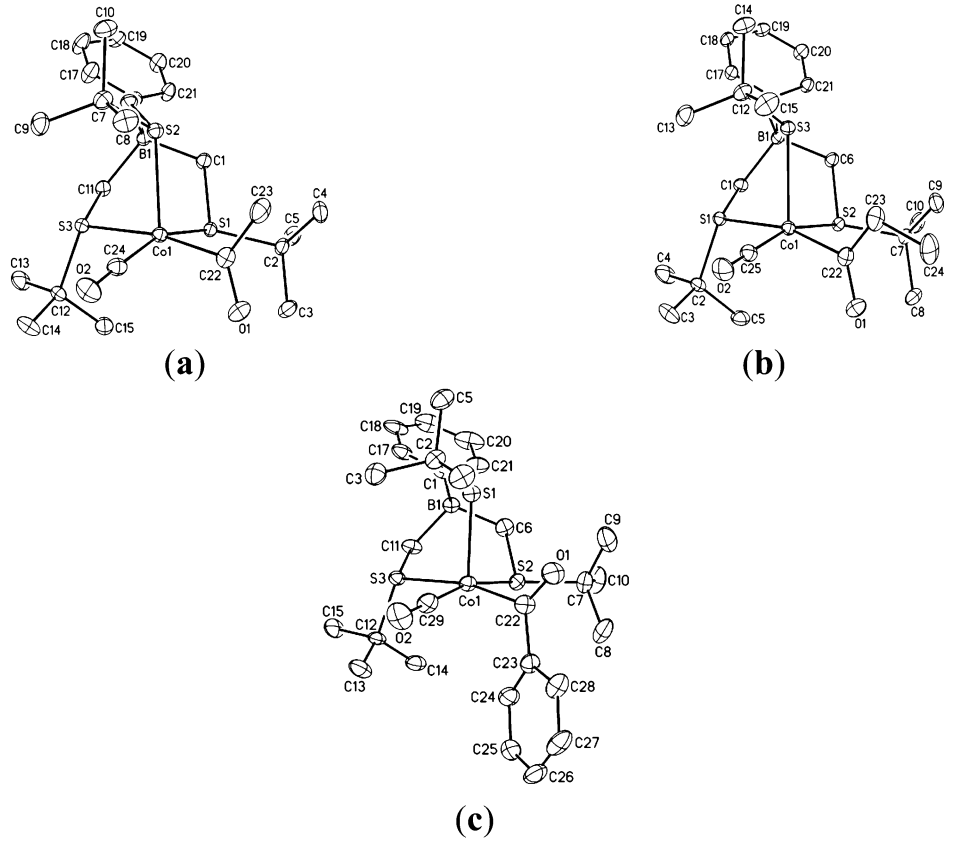

Figure 3. Thermal ellipsoid plots of (a) [PhTt^{tBu}]Co(CO)(C(O)Me), (b) [PhTt^{tBu}]Co(CO)(C(O)Et), and (c) [PhTt^{tBu}]Co(CO)(C(O)Ph). Thermal ellipsoids are drawn at 30% probability. Hydrogen atoms have been omitted for clarity.

Table 4. Selected Bond Lengths and Bond Angles for [PhTt^{tBu}]Co(CO)(C(O)Me), [PhTt^{tBu}]Co(CO)(C(O)Et), and [PhTt^{tBu}]Co(CO)(C(O)Ph)

	length (Å)		angle (deg)
	[PhTt^{tBu}]Co(CO)(C(O)Me) (**7**)		
Co−C(22)	1.946(2)	C(24)−Co−C(22)	83.10(9)
Co−C(24)	1.774(2)	C(24)−Co−S(2)	103.58(7)
Co−S(1)	2.3205(6)	C(22)−Co−S(2)	100.63(6)
Co−S(2)	2.3669(5)	S(1)−Co−S(2)	96.37(1)
Co−S(3)	2.3684(5)	S(3)−Co−S(2)	88.34(1)
	[PhTt^{tBu}]Co(CO)(C(O)Et) (**8**)		
Co−C(22)	1.941(1)	C(25)−Co−C(22)	81.20(7)
Co−C(25)	1.775(1)	C(25)−Co−S(3)	101.11(5)
Co−S(1)	2.3663(4)	C(22)−Co−S(3)	104.14(4)
Co−S(2)	2.3363(4)	S(1)−Co−S(3)	89.34(1)
Co−S(3)	2.3719(4)	S(2)−Co−(3)	94.92(1)
	[PhTt^{tBu}]Co(CO)(C(O)Ph) (**9**)		
Co−C(22)	1.959(5)	C(29)−Co−C(22)	82.0(2)
Co−C(29)	1.765(6)	C(29)−Co−S(1)	103.6(2)
Co−S(1)	2.3051(1)	C(22)−Co−S(1)	100.8(1)
Co−S(2)	2.279(1)	S(2)−Co−S(1)	91.46(6)
Co−S(3)	2.342(1)	S(3)−Co−S(1)	91.22(5)

Scheme 3. Synthesis of [PhTt^{tBu}]Co(CO)$_2$

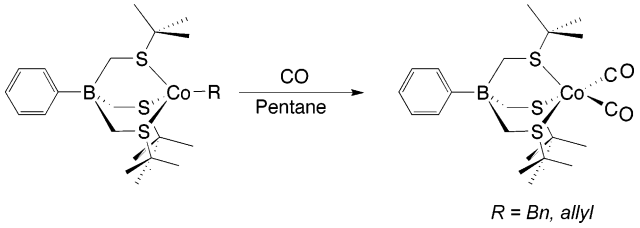

and rigidness of the [Tp^{tBu}] ligand, which does not permit the formation of a five-coordinate complex requisite for CO insertion. This observation is in contrast to our results in that the Co−Me bond dissociation energy is expected to be significant, due to the high energy of the methyl radical.

A reasonable mechanism for formation of [PhTt^{tBu}]Co(CO)$_2$ can be proposed on the basis of the reactivity noted for [PhTt^{tBu}]Co(R) (R = Me, Et, Ph) coupled with the observation that carbonylation of [Tp^{iPr2}]Co(R′) (R′ = C_3H_5, *p*-methylbenzyl)[8] resulted in the formation of a five-coordinate acyl/carbonyl intermediate. [PhTt^{tBu}]Co(CO)$_2$ most likely forms via addition of CO followed by homolytic rupture of the Co−C bond of the benzyl or allyl moiety. The resulting [PhTt^{tBu}]Co(CO) complex is trapped by additional CO, yielding the observed product. Indeed, independent evidence for [PhTt^{tBu}]Co(CO) has been obtained, vide infra.

A thermal ellipsoid representation of [PhTt^{tBu}]Co(CO)$_2$ is contained in Figure 4a with selected metric parameters in Table 4. The Co$^+$ lies in a square pyramidal geometry ($\tau = 0.24$)[20] with the carbonyl ligands occupying the basal plane with two thioethers; the remaining thioether is in the apical position. The Co−C bond distances of 1.742(4) and 1.757(4) Å are comparable to those found for other neutral Co$^+$ species, i.e., [Tp^{Np}]Co(CO),[11] 1.769(5) Å, and [PhBP$_3$]Co(CO)$_2$,[21] 1.729(5) and 1.744(5) Å.

Surprisingly, FTIR analysis of [PhTt^{tBu}]Co(CO)$_2$ in pentane solution indicated multiple species present as revealed by three ν_{CO} modes at 2015, 1966, and 1949 cm^{-1}. The absorptions at 2015 and 1949 cm^{-1} were significantly more intense than the 1966 cm^{-1} band. The former are assigned to the symmetric and asymmetric ν_{CO} modes, respectively, of [PhTt^{tBu}]Co(CO)$_2$. These two ν_{CO} modes are observed at lower energy in [PhBP$_3$]Co(CO)$_2$,[21] displaying symmetric and symmetric stretches at

(21) Jenkins, D. M.; Betley, T. A.; Peters, J. C. *J. Am. Chem. Soc.* **2002**, *124*, 11238.

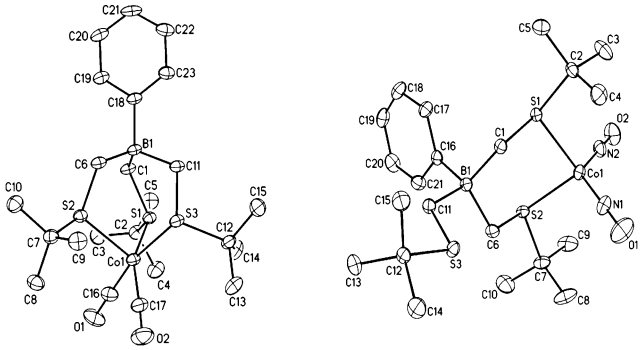

Figure 4. Thermal ellipsoid plots of (a) [PhTt^{tBu}]Co(CO)$_2$ and (b) [κ^2-PhTt^{tBu}]Co(NO)$_2$. Thermal ellipsoids are drawn at 30% probability. Hydrogen atoms have been omitted for clarity.

Scheme 4. Equilibrium between [PhTt^{tBu}]Co(CO)$_2$ and [PhTt^{tBu}]Co(CO)

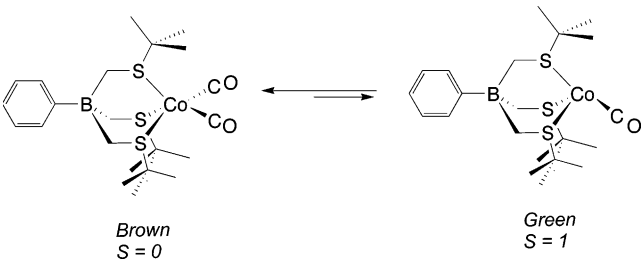

2008 and 1939 cm^{-1}. The ν_{CO} mode at 1966 cm^{-1} is ascribed to the monocarbonyl species [PhTt^{tBu}]Co(CO), Scheme 4. This absorption band is of similar energy to those reported for the monocarbonyl species [Tp^{iPr2}]Co(CO)[8] and [Tp^{Np}]Co(CO),[11] each displaying a ν_{CO} stretch at 1950 cm^{-1}. These observations further establish that the [PhBP$_3$], [Tp^{iPr2}], and [Tp^{Np}] tripods are more electron releasing than [PhTt^{tBu}].

To assess the likelihood that [PhTt^{tBu}]Co(CO) and [PhTt^{tBu}]Co(CO)$_2$ are in equilibrium, a pentane solution of [PhTt^{tBu}]Co(CO)$_2$ was subjected to multiple freeze/pump/thaw cycles in an effort to drive the equilibrium toward [PhTt^{tBu}]Co(CO). Following each cycle, the dicarbonyl bands at 2015 and 1949 cm^{-1} diminished in intensity while the monocarbonyl stretch (1966 cm^{-1}) became more prominent. This process is reversible, as addition of CO to a solution of the monocarbonyl species results in re-formation of [PhTt^{tBu}]Co(CO)$_2$.

The identification of [PhTt^{tBu}]Co(CO) was corroborated further via proton NMR spectroscopy. Analogous to the infrared experiment, [PhTt^{tBu}]Co(CO)$_2$ was subjected to multiple freeze/pump/thaw sequences, during which the solution color changed from brown to green. The NMR spectrum of the green species revealed a number of paramagnetically shifted resonances. [PhTt^{tBu}]Co(CO)$_2$ is diamagnetic. The *tert*-butyl protons resonate at δ −1.54, while the methylene proton resonance is a broad feature centered at δ 156.3. These spectral characteristics are akin to those observed for other monovalent cobalt and nickel [PhTt^{tBu}]M(L) complexes prepared in these laboratories.[4,22] Efforts to crystallize [PhTt^{tBu}]Co(CO) led only to isolation of brown crystals of [PhTt^{tBu}]Co(CO)$_2$.

Reactivity of [PhTt^{tBu}]Co(R) Complexes with NO (R = Me, Et, Ph, Bn, allyl). The organocobalt complexes [PhTt^{tBu}]Co(R) (R = Cl, Me, Et, Ph, Bn, allyl) were reacted with 1 atm NO in pentane solution. In all cases, a rapid color change to brown was apparent immediately. Removal of the solvent and extraction of the product with diethyl ether led to the isolation of [κ^2-PhTt^{tBu}]Co(NO)$_2$. Crystals appropriate for X-ray diffraction analysis were grown from a concentrated pentane solution. A thermal ellipsoid representation and selected bond lengths and angles are contained in Figure 4b and Table 5, respectively. The cobalt is in a tetrahedral ligand environment formed by two of the thioether donors and two nitrosyl ligands. The Co−S distances of 2.2746(6) and 2.2828(6) Å compare well to the average Ni−S distance of 2.2843(7) Å found for the [PhTt^{tBu}]Ni(NO). The Co−N distances of 1.661(3) and 1.671(2) Å are comparable to those found for [Tp^{tBu,Me}]Co(NO) of 1.671(7) Å. The Co−N−O angles of 179.0(3)° and 178.8(2)° indicate linear nitrosyl ligation. This geometry is consistent with the NO$^+$ formalism, the diatomic donor isoelectronic with CO. Using the preferred Enemark−Feltham notation the Co(NO)$_2$ moiety is designated {Co(NO)$_2$}^{10}.[23,24] On the basis of similar transformations observed in transition metal nitrosyl complexes,[24,25] it is expected that the R (or Cl) lost upon addition of NO forms the corresponding RNO or NOCl byproducts via reaction with excess NO. These species were not detected.

Table 5. Selected Bond Lengths and Bond Angles for [PhTt^{tBu}]Co(CO)$_2$ and [κ^2-PhTt^{tBu}]Co(NO)$_2$

	length (Å)		angle (deg)
	[PhTt^{tBu}]Co(CO)$_2$ (**10**)		
Co−C(16)	1.742(4)	C(16)−Co−C(17)	85.0(2)
Co−C(17)	1.757(4)	C(16)−Co−S(2)	99.0(1)
Co−S(1)	2.292(2)	C(17)−Co−S(2)	111.91(1)
Co−S(2)	2.354(2)	S(1)−Co−S(2)	94.1(1)
Co−S(3)	2.303(3)	S(3)−Co−S(2)	92.4(1)
	[κ^2-PhTt^{tBu}]Co(NO)$_2$ (**12**)		
Co−N(1)	1.661(3)	N(1)−Co−N(2)	129.0(1)
Co−N(2)	1.671(2)	N(2)−CoS(1)	106.5(1)
Co−S(1)	2.2828(6)	N(1)−Co−S(2)	108.31(8)
Co−S(2)	2.746(6)	S(1)−Co−S(2)	91.32(2)

The proton NMR spectrum of [κ^2-PhTt^{tBu}]Co(NO)$_2$ is consistent with a $S = 0$ ground state. Although the thioether ligand is bound in a κ^2-fashion, a single set of *tert*-butyl proton resonances is apparent, δ 1.15, on the NMR time scale.

The infrared spectrum of [κ^2-PhTt^{tBu}]Co(NO)$_2$ revealed two ν_{NO} modes at 1846 and 1789 cm^{-1}, which were assigned as the symmetric and asymmetric ν_{NO} bands, respectively. These data are comparable to those reported for other crystallographically characterized {Co(NO)$_2$} fragments. For example, the ν_{NO} modes for [Co(NO)$_2$Cl]$_2$[24] are at 1859 and 1790 cm^{-1} and for [Co(NO)$_2$I]$_x$, at 1846 and 1792 cm^{-1}.[25]

Transition metal nitrosyl complexes have been extensively reviewed in the literature.[26] The bridging nitrosyl complex [CpCoNO]$_2$ reacts with alkenes to yield the corresponding dinitrosoalkanes.[27] Bergman and co-workers investigated this reaction and showed kinetic and spectroscopic evidence for a reactive intermediate, CpCo(NO)$_2$.[27] Theopold and co-workers have reported a cobalt mononitrosyl derivative, [Tp^{tBu,Me}]Co(NO).[28] In addition, within the [PhTt^{tBu}] ligand family, blue [PhTt^{tBu}]Ni(NO) was synthesized by reaction of [PhTt^{tBu}]NiCl with excess NO. Parkin observed an interesting tridentate to

(22) DuPont, J. A. *The Coordination Chemistry of Thioether-supported, Low-valent Cobalt Complexes*; University of Delaware: Newark, DE, 2005.
(23) Enemark, J. H.; Feltham, R. D. *Coord. Chem. Rev.* **1974**, *13*, 339.
(24) Hayton, T. W.; Legzdins, P.; Patrick, B. O. *Inorg. Chem.* **2002**, *41*, 5388.
(25) Dahl, L. F.; deGil, E. R.; Feltham, R. D. *J. Am. Chem. Soc.* **1969**, *91*, 1653.
(26) Richter-Addo, G. B.; Legzdins, P. *Metal Nitrosyls*; Oxford University Press: New York, 1992.
(27) Becker, P. N.; Bergman, R. G. *J. Am. Chem. Soc.* **1983**, *105*, 2985.
(28) Thyagarajan, S.; Shay, D. T.; Incarvito, C. D.; Rheingold, A. L.; Theopold, K. H. *J. Am. Chem. Soc.* **2003**, *125*, 4440.

bidentate conversion of the [Tp^{tBu}] ligand upon reaction of [Tp^{tBu}]Fe(Me) with NO to form [κ^2-Tp^{tBu}]Fe(NO)$_2$.[29]

Conclusions

A series of alkyl and aryl organocobalt(II) species [PhTt^{tBu}]-Co(R) were synthesized and characterized. When R = Me, Et, Ph, or Bn, the resultant complexes are high-spin 15-electron species. By contrast, the allyl derivative is a low-spin, square pyramidal complex with the allyl ligand acting as a four-electron donor. While these organocobalt(II) complexes are electronically and coordinatively unsaturated, they are inherently stable at ambient temperature in the absence of moisture and dioxygen; similar observations having been made for the related [Tp^R]-Co(R) species. The reactivity of [PhTt^{tBu}]Co(R) with CO and NO revealed that the outcome of the carbonylation reactions was dependent on the identity of the organic ligand, whereas the NO reactions were not. This differential CO reactivity between the benzyl/allyl derivatives and the other organocobalt species is rationalized by differences in relative cobalt−carbon bond strengths. The benzyl and allyl moieties are substituted readily by CO, due to the stability of the corresponding radical, R$^\bullet$. This process is presumed to be associative, in part because the reactions with CO are rapid. Cobalt−carbon bond homolysis renders the metal fragment formally reduced and susceptible to ligand trapping. Indeed, this strategy represents an attractive synthetic approach for the synthesis of monovalent cobalt complexes. The methyl, ethyl, and phenyl ligands, however, form more robust cobalt−carbon bonds,[30] leading to products resulting from CO insertion.

Experimental Section

Materials and Methods. Unless otherwise noted, all reactions were carried out under an inert atmosphere of N_2 using standard Schlenk line techniques or in an argon-filled Vacuum Atmospheres glovebox equipped with a gas purification system.[31] All glassware was dried at 140 °C for at least 4 h. Solvents were dried by passing through a column of activated alumina, followed by thorough degassing with N_2. Water and peroxides were removed from 1,4-dioxane by refluxing with $NaBH_4$, followed by distillation under N_2, and stored over 4 Å molecular sieves. All Grignard reagents were purchased from Acros Organics and used as received. Carbon monoxide was purchased from Keen Gas and dried by passage through successive columns of Drierite and 4 Å molecular sieves. Nitric oxide was purified stepwise by purging through 12 M sodium hydroxide, calcium sulfate, and phosphorus pentaoxide.[32] [PhTt^{tBu}]-Tl, [PhTt^{tBu}]CoCl, and [PhTt^{tBu}]NiCl were prepared according to previously published procedures.[33] Deuterated solvents were purchased from Cambridge Isotope Laboratories and dried over 4 Å molecular sieves.

Proton and ^{13}C NMR spectra were recorded on either a Bruker 360 MHz spectrometer equipped with a Sun Workstation, a Bruker AM 250 MHz, or a Bruker AC 250 MHz spectrometer. All NMR signals were referenced to residual protio solvent signals. Unless otherwise noted, all data were collected at ambient temperature. Chemical shifts are quoted in δ (ppm) and coupling constants in hertz. Abbreviations are as follows: s, singlet; d, doublet; t, triplet; q, quartet; m, multiplet; br, broad. Magnetic moments were determined in solution via the Evans method.[34] Electronic spectra were recorded a Hewlett-Packard 8453 diode array spectrometer. Infrared spectra were recorded on a Mattson Genesis Series FTIR spectrometer under N_2 purge at ambient temperature. Solid-state FT-IR samples were prepared as KBr pellets and solution-state FT-IR samples were prepared in pentane using KBr disks and a Thermo sample cell holder. Melting points were determined with a Melt-Temp melting point determination apparatus and are reported uncorrected. Elemental analyses were performed by Desert Analytics, Inc., Tucson, AZ, Galbraith Laboratory, Inc., Knoxville, TN, or Oneida Research Services, Inc., Whitesboro, NY.

Single-Crystal X-ray Diffraction Studies. Crystals were selected and mounted on glass fibers with either epoxy or cryogenically cooled viscous oil. Crystallographic data were collected on a Bruker-AXS APEX diffractometer. Minimum/maximum transmission ratios for **1**, **6**, and **10** were near unity, and no absorption corrections were applied. All other data sets were treated with SADABS absorption corrections. No symmetry higher than triclinic was observed in the diffraction data for **7** and **8**. The structural solutions in the centrosymmetric space group option yielded chemically reasonable and computationally stable results of refinement. Systematic absences and unit-cell parameters were uniquely consistent for the reported space group for the other compounds. The sulfur atoms in **5** were disordered in two positions with refined site occupancy of 87/13. All non-hydrogen atoms were refined with anisotropic displacement parameters. Hydrogen atoms were treated as idealized contributions. All software and sources of the scattering factors are contained in various versions of the SHELXTL program library (G. Sheldrick; Siemens XRD, Madison, WI). Structures have been deposited at the Cambridge Structural Database under depository numbers CCDC 618937 to 618945.

[κ^2-PhTt^{tBu}]Ni(η^3-allyl) (1). [PhTt^{tBu}]NiCl (100 mg, 0.204 mmol) was dissolved in 10 mL of THF. The volume was increased to 50 mL by addition of 1,4-dioxane. Two equivalents of allylMgBr was added dropwise via syringe. An immediate color change from red to yellow was noted. The solution was stirred at room temperature for 8 h. The solution was filtered through Celite on a medium-porosity filter. The filtrate was collected and solvent removed under reduced pressure with gentle heating (≤60°). The product was extracted with pentane and passed through a Celite plug to remove any impurities. [κ^2-PhTt^{tBu}]Ni(η^3-allyl) was crystallized from a concentrated ethyl ether solution at room temperature. Yield: 47 mg, 42%. MP: 107 °C (dec). ^{1}H NMR (C_6D_6): δ 7.89 (2 H, s, *m*-(C_6H_5)B), 7.28 (1 H, m, *p*-(C_6H_5)B), 7.15 (2 H, s, *o*-(C_6H_5)B), 4.50 (1 H, m, ^3J 7.45 Hz, central C*H*), 3.30−3.22 (2 H, m, ^3J 6.83 Hz, *syn*-CH_2), and 3.04−3.02 (2 H, d, ^3J 6.75 Hz, *anti*-CH_2), 1.25 (27 H, br, (CH_3)$_3$S). ^{13}C NMR (C_6D_6): δ 134.5 (*o*-(C_6H_5)B), 133.3 (*p*-(C_6H_5)B), 127.3 (*m*-(C_6H_5)B), 108.8 (*anti*-CH_2), 59.7 (*syn*-CH_2), 44.6 (CH_2), 30.3 (CH_3)$_3$S), 14.6 (C(CH$_3$)$_3$). UV−vis (pentane), λ_{max} (ϵ, M^{-1} cm^{-1}): 323 (213), 387 (99), 426 (85). Anal. Calcd for $C_{24}H_{43}S_3BNi$: C, 57.9; H, 8.71. Found: C, 57.7; H, 8.54.

[PhTt^{tBu}]Co(R) Complexes (R = Me, Et, Ph, Bn, allyl). [PhTt^{tBu}]CoCl (100 mg, 0.2 mmol) was dissolved in 10 mL of dry THF. The volume was then increased to 50 mL by addition of 1,4-dioxane. Two equivalents of the appropriate Grignard reagent were added dropwise via syringe to the stirring solution. The reaction was stirred at room temperature under an inert atmosphere for 8 h. The solution was then filtered through Celite on a medium-porosity filter. The filtrate was collected and the solvent was removed under reduced pressure with gentle heating (≤60 °C). The product was then extracted with pentane and passed through a Celite plug to remove any impurities.

[PhTt^{tBu}]Co(Me) (2).[4] Yield: 75 mg (78%). Mp: 110 °C (dec). ^{1}H NMR (C_6D_6): δ 18.8 (br, 2 H, *o*-(C_6H_5)B), 10.8 (br, 2 H,

(29) Kisko, J. L.; Hascall, T.; Parkin, G. *J. Am. Chem. Soc.* **1998**, *120*, 10561.
(30) Halpern, J. *Polyhedron* **1988**, *7*, 1483.
(31) Shriver, D. F.; Drezdon, M. A. *The Manipulation of Air Sensitive Compounds*, 2nd ed.; Wiley: New York, 1986.
(32) Perrin, D.; Armarego, W. L. F. *Purification of Laboratory Chemicals*, 3rd ed.; Pergamon: New York, 1988.
(33) Schebler, P. J.; Riordan, C. G.; Guzei, I.; Rheingold, A. L. *Inorg. Chem.* **1998**, *37*, 4754.
(34) Drago, R. S. *Physical Methods for Chemists*, 2nd ed.; Saunders College Publishing: New York, 1992.

m-(C_6H_5)B), 9.8 (br, 1 H, *p*-(C_6H_5)B), 3.13 (br, 27H, (CH_3)$_3$S). μ_{eff} (C_6D_6) = 5.1 μ_B. UV−vis (pentane), λ_{max} (ϵ, M^{-1} cm^{-1}): 632 (570), 725 (574). Anal. Calcd for $C_{22}H_{41}S_3BCo$: C, 56.0; H, 8.77. Found: C, 55.2; H, 8.60.

[PhTt^{tBu}]Co(Et) (3). Yield: 70 mg (71%). Mp: 108 °C (dec). ^{1}H NMR (C_6D_6): δ 19.9 (br, 2 H, *o*-(C_6H_5)B), 11.2 (br, 2 H, *m*-(C_6H_5)B), 10.3 (br, 1 H, *p*-C_6H_5)B), 1.22 (br, 27 H, (CH_3)$_3$S), −9.36 (2 H, br, −CH_3). μ_{eff} (C_6D_6) = 4.1 μ_B. UV−vis (pentane), λ_{max} (ϵ, M^{-1} cm^{-1}): 609 (443), 740 (830). Anal. Calcd for $C_{23}H_{43}S_3$-BCo: C, 56.9; H, 8.93. Found: C, 57.0; H, 8.70.

[PhTt^{tBu}]Co(Ph) (4). Yield: 68 mg (63%). Mp: 105 °C (dec). ^{1}H NMR (C_6D_6): δ 40.4 (2 H, br, *m*-(C_6H_5)Co), 19.5 (br, 2 H, *o*-(C_6H_5)B), 11.0 (br, 2 H, *m*-(C_6H_5)B), 10.2 (br, 1 H, *p*-(C_6H_5)B), 3.35 (br, 27 H, (CH_3)$_3$S), −20.9 (1 H, br, *p*-(C_6H_5)Co), −26.5 (2 H, br, *o*-(C_6H_5)Co). μ_{eff} (C_6D_6) = 4.2 μ_B. UV−vis (pentane), λ_{max} (ϵ, M^{-1} cm^{-1}): 643 (249), 719 (359), 743 (578). Anal. Calcd for $C_{27}H_{43}S_3BCo$: C, 60.7; H, 8.12. Found: C, 60.6; H, 7.91.

[PhTt^{tBu}]Co(Bn) (5). Yield: 60 mg (55%). Mp: 98 °C. ^{1}H NMR (C_6D_6): δ 46.2 (2 H, s, *m*-(C_6H_5)), 19.3 (2 H, br, *o*-(C_6H_5)B), 11.2 (1 H, *s*, *p*-(C_6H_5)B), 10.3 (2 H, *s*, *m*-(C_6H_5)B), 2.52 (27 H, br, (CH_3)$_3$S), −93.1 (2 H, br, *o*-(C_6H_5)), −110.8 (1H, br, *p*-(C_6H_5)). μ_{eff} (C_6D_6) = 3.8 μ_B. UV−vis (pentane), λ_{max} (ϵ, M^{-1} cm^{-1}): 511 (682), 655 (346), 711 (258), 761 (430). Anal. Calcd for $C_{28}H_{45}S_3$-BCo: C, 61.4; H, 8.29. Found: C, 59.0; H, 7.52. *Samples prepared in independent syntheses repeatedly tested low in carbon analyses.*

[PhTt^{tBu}]Co(η^3-allyl) (6). Yield: 63 mg (62%). Mp: 94 °C (dec). ^{1}H NMR (C_6D_6): δ 10.0 (2 H, br, *o*-C_6H_5)B), 8.49 (2H, br, *m*-C_6H_5)B), 7.99 (1 H, br, *p*-C_6H_5)B), 1.37 (27 H, br, (CH_3)$_3$S). μ_{eff} (C_6D_6) = 2.5 μ_B. UV−vis (pentane), λ_{max} (ϵ, M^{-1} cm^{-1}): 407 (1227), 716 (271). Anal. Calcd for $C_{24}H_{43}S_3BCo$: C, 57.9; H, 8.72. Found: C, 57.7; H, 8.99.

Synthesis of [PhTt^{tBu}]Co(CO)(C(O)R) (R = Me, Et, Ph). Dry CO was passed through a pentane solution (10 mL) containing 50 mg of [PhTt^{tBu}]Co(R) at room temperature for ∼2 min. An immediate color change from green to red was apparent. Solvent was removed in vacuo, yielding a red solid in high yields (80−90%). Crystals appropriate for X-ray analysis were grown by slow evaporation of a concentrated pentane solution.

[PhTt^{tBu}]Co(CO)(C(O)Me) (7). Yield: 50 mg, 90%. Mp: 91 °C (dec). ^{1}H NMR (C_6D_6): δ 9.07 (2 H, br, *o*-C_6H_5)B), 8.10 (1 H, br, *p*-C_6H_5)B), 8.01 (2 H, br, *m*-C_6H_5)B), 3.91 (27 H, br, (CH_3)$_3$S), 0.99 (3 H, br, (CO)CH_3). μ_{eff} (C_6D_6) = 2.0 μ_B. UV−vis (pentane), λ_{max} (ϵ, M^{-1} cm^{-1}): 555 (420), 689 (175), 914 (161). FTIR (pentane): 1997 (ν_{CO}), 1686, 1665 (ν_{COR}) cm^{-1}. Anal. Calcd for $C_{24}H_{41}S_3O_2BCo$: C, 54.6; H, 7.83. Found: C, 53.9; H, 7.65.

[PhTt^{tBu}]Co(CO)(C(O)Et) (8). Yield: 50 mg, 90%. Mp: 88 °C (dec). ^{1}H NMR (C_6D_6): δ 8.90 (2 H, br, *o*-(C_6H_5)B), 7.81 (2 H, br, *m*-(C_6H_5)B), 6.37 (1 H, br, *p*-(C_6H_5)B), 3.30 (27 H, br, C(CH_3)$_3$S). μ_{eff} (C_6D_6) = 1.9 μ_B. UV−vis (pentane), λ_{max} (ϵ, M^{-1} cm^{-1}): 531 (58), 677 (26), 912 (17). FTIR (pentane): 1995 (ν_{CO}), 1658 (ν_{COR}) cm^{-1}. Anal. Calcd for $C_{25}H_{43}S_3BCo$: C: 55.4, H, 8.00. Found: C, 52.1; H, 7.64. *Samples prepared in independent syntheses repeatedly tested low in carbon analyses.*

[PhTt^{tBu}]Co(CO)(C(O)Ph) (9). Yield: 45 mg, 81%. ^{1}H NMR (C_6D_6): δ 26.9 (br, 2 H, *m*-(C_6H_5)), 10.53 (br, 2 H, *o*-(C_6H_5)B), 8.45 (br, 2 H, *m*-(C_6H_5)B), 7.96 (br, 1 H, *p*-(C_6H_5)B), 5.79 (br, 27 H, C(CH_3)$_3$S), -13.63 (br, 1 H, *p*-(C_6H_5)), -19.9 (br, 2 H, *o*-(C_6H_5)). μ_{eff} (C_6D_6) = 2.1 μ_B UV−vis (pentane), λ_{max} (ϵ, M^{-1} cm^{-1}): 495 (213), 528 (224), 734 (91). FTIR (pentane): 2002 (ν_{CO}), 1709 (ν_{COR}) cm^{-1}.

Synthesis of [PhTt^{tBu}]Co(CO)$_2$ (10). Dry CO was passed through a pentane solution (10 mL) containing 50 mg of the [PhTt^{tBu}]Co(R) complex at room temperature for ∼2 min. An immediate color change from purple (R = Bn) or orange (R = allyl) to brown was apparent. Solvent was removed in vacuo, yielding a brown solid, [PhTt^{tBu}]Co(CO)$_2$. Crystals appropriate for X-ray diffraction analysis were grown by slow evaporation from a concentrated pentane solution. Yield: 44 mg, 85%. Mp: 127 °C (dec). ^{1}H NMR (C_6D_6): δ 7.68 (2 H, br, *o*-(C_6H_5)B), 7.48 (2 H, br, *m*-(C_6H_5)B), 7.29 (1 H, br, *p*-(C_6H_5)B), 2.05 (5 H, −CH_2), 1.34 (27 H, br, (CH_3)$_3$S). ^{13}C NMR (C_6D_6): δ 206.6 (*C*O), 132.1 (*o*-(C_6H_5)B), 131.6 (*p*-(C_6H_5)B), 125.2 (*m*-(C_6H_5)B), 48.1 (CH_2), 29.1 ((CH_3)$_3$S), 14.6 (C(CH_3)$_3$). UV−vis (pentane), λ_{max} (ϵ, M^{-1} cm^{-1}): 407 (473), 658 (168). FTIR (pentane): 2015, 1949 (ν_{CO}) cm^{-1}. Anal. Calcd for $C_{23}H_{38}S_3BCoO_2$: C, 53.9; H, 7.48. Found: C, 55.1; H, 8.32.

Synthesis of [PhTt^{tBu}]Co(CO) (11). Exposing solutions (pentane or C_6D_6) of [PhTt^{tBu}]Co(CO)$_2$ to multiple freeze−pump−thaw cycles resulted in a color change from brown to green. This process was fully reversible. In situ spectroscopic interrogation of the green solutions revealed formation of [PhTt^{tBu}]Co(CO). ^{1}H NMR (C_6D_6): δ 156.3 (6 H, br, (CH_2)), 18.4 (s, 2 H, *m*-(C_6H_5)B), 10.7 (s, 2 H, *o*-(C_6H_5)B), 10.6 (s, 1 H, *p*-(C_6H_5)B), FTIR (pentane): 1966 (ν_{CO}) cm^{-1}.

Reaction of [PhTt^{tBu}]Co(R) Complexes with NO (R = Me, Et, Ph, Bn, allyl); Synthesis of [κ^2-PhTt^{tBu}]Co(NO)$_2$ (12). Dry NO was passed through a pentane solution (10 mL) containing 50 mg of the [PhTt^{tBu}]Co(R) for ∼2 min. An immediate color change to brown was apparent. The solvent was removed under reduced pressure, and the product was extracted with diethyl ether. Crystals were grown by slow evaporation from a concentrated ethyl ether solution. Yield: 44 mg, 80%. ^{1}H NMR (C_6D_6): δ 7.89 (2 H, br, *m*-(C_6H_5)B), 7.52 (2 H, br, *o*-(C_6H_5)B), 7.15 (1 H, br, *p*-(C_6H_5)B), 2.39 (6 H, s, (CH_2)), 1.15 (27 H, br, (CH_3)$_3$S). FTIR (pentane): 1846, 1789 (ν_{NO}) cm^{-1}. Anal. Calcd for $C_{21}H_{38}S_3N_2O_2BCo$: C, 48.8; H, 7.41; N, 5.43. Found: C, 45.9; H, 7.42; N, 5.70. *Samples prepared in independent syntheses repeatedly tested low in carbon analyses.*

Acknowledgment. This work was funded by the National Science Foundation (CHE-0213260).

Supporting Information Available: CIF files for all X-ray structures. This material is available free of charge via the Internet at http://pubs.acs.org.

OM0608253